Vol. 23, No. 3(2024) Mat24264
Revista Mexicana de Ingeniería Química

Structural and chemical analysis of Zn ion exchange in thermally modified zeolite A4

Análisis estructural y químico del intercambio iónico de Zn en zeolita A4 modificada térmicamente

J.E. Leal-Perez[1], J. L. Almaral-Sanchez[1], A. Hurtado-Macias[2], M. Cortez-Valadez[3], A. Bórquez-Mendívil[1], B. A. García-Grajeda[1], J. M. Mendivil-Escalante[1], J. Flores-Valenzuela[1]*

[1] *Universidad Autónoma de Sinaloa, Fuente de Poseidón y Prol., Ángel Flores S/N, C.P.81223, Los Mochis, Sinaloa, México.*

[2] *Department of Metallurgy and Structural Integrity, National Nanotechnology Laboratory Centro de Investigación en Materiales Avanzados S.C., Chihuahua, Chihuahua, México.*

[3] *CONACYT-Departamento de Investigación en Física, Universidad de Sonora, Apdo. Postal 5-88, Hermosillo, Sonora 83190, México.*

Received: February 8, 2024; Accepted: April 11, 2024

Abstract

This work reports the analysis of Zn ion exchange in thermally modified zeolite A4 (ZA4) for the potential formation of ZnO nanoparticles. The methodology consists of two steps. Step 1 consisted of carrying out different thermal treatments on ZA4. Step 2 involved the ion exchange of Zn with different concentrations of the Zn ion precursor. XRD and FTIR analyses revealed a transformation in the crystal and molecular structure of ZA4 after heat treatment. This work has been limited to studying ion exchange; however, it is very interesting to study the thermal behavior of ZA4 because this could improve the surface area of the material. The results obtained in this work demonstrate that heat treatment and Zn ion concentration affect the crystallinity and molecular structure of ZA4.

Keywords: Zn, zeolite A4, heat treatment, structural analysis.

Resumen

Este trabajo reporta el análisis del intercambio de iones de Zn en la zeolita A4 modificada térmicamente (ZA4) para la potencial formación de nanopartículas de ZnO. La metodología realizada, consta de un proceso de 2 etapas. La etapa 1 consistió en realizar diferentes tratamientos térmicos en ZA4. La etapa 2 involucró el intercambio iónico de Zn con diferentes concentraciones del precursor de iones Zn. Los análisis por DRX y FTIR muestran una transformación en la estructura cristalina y molecular de ZA4 después de los tratamientos. Este trabajo se ha limitado al estudio del intercambio iónico, sin embargo, resulta muy interesante conocer el comportamiento térmico de ZA4, ya que esto, puede favorecer el área superficial del material. Los resultados obtenidos en este trabajo demuestran que el tratamiento térmico y la concentración de iones Zn afectan la estructura cristalina y molecular de ZA4.

Palabras clave: Zn, zeolita A4, tratamiento térmico, análisis estructural.

* *Corresponding author. E-mail*: jflores@uas.edu.mx;
https://doi.org/10.24275/rmiq/Mat24264
ISSN:1665-2738, *issn-e*: 2395-8472

1 Introduction

Zeolites consist of $[SiO_4]^{4-}$ and $[AlO_4]^{5-}$ tetrahedral frameworks connected at vertices by oxygen atoms, with group I and II elements as exchange ions. The high selective adsorption capacity of ions is their main characteristic (Eroglu, Emekci, & Athanassiou, 2017; Leal-Perez, Flores-Valenzuela, Cortez-Valadez, et al., 2022). In particular, Zeolite Linde Type A (Zeolite LTA or Zeolite A) was the first synthetic zeolite commercially available (Breck, Eversole, & Milton, 1956). The general formula of LTA zeolite is $X_{12}[(AlO_2)_{12}(SiO_2)_{12}]\cdot 27H_2O$, where X could be K, Na or Ca (for Ca, 12 is changed by 6 due to the valence electrons), which are referred to as zeolites A3, A4, and A5, respectively. Moreover, the ratio of structural silicon to aluminum (Si/Al) is 1, and sodium ions are exchangeable structural cations (Julbe & Drobek, 2016). The fact that LTA zeolite has a Si/Al ratio equal to 1 means that it potentially has a high cation exchange capacity (Collins, Rozhkovskaya, Outram, & Millar, 2020).

Ion exchange in zeolites is a metathesis reaction (double displacement reaction) between the zeolite and a specific salt, where a specific reaction occurs between the cations of both species (Hoveyda & Zhugralin, 2007; Leal-Perez, Flores-Valenzuela, Vargas-Ortíz, et al., 2022). One of the first ion exchange researchers studying zeolites was Eichhorn, who reported that this type of reaction was reversible (Eichhorn, 1858). However, no industrial applications of this process are available, and for several years, zeolites were considered to have simple mineralogical curiosities. However, around the 1950s, important deposits were discovered in Japan, Italy, and the United States. After that, zeolites (called ion exchange resins) became the main product for solving problems related to water softening and deionization within a few years (Colella, 1996; Gans, 1905).

On the other hand, the ion exchange of Zn in a zeolite can offer a promising precursor for the formation of ZnO nanoparticles. A controlled size and homogeneous distribution were demonstrated for other nanoparticles synthesized from zeolites (Leal-Perez, Flores-Valenzuela, Vargas-Ortíz, et al., 2022). Zinc oxide (ZnO) is a semiconductor with a band gap of 3.37 eV at room temperature. Different physical and chemical properties can be obtained depending on the nanostructure morphology (Reyes-Zambrano, Lecona-Guzmán, Luján-Hidalgo, & Gutiérrez-Miceli, 2024). For this purpose, ZnO is considered a technologically relevant material with a variety of applications, such as semiconductors, sensors, magnetic and actuator materials, and cosmetic ingredients (Hasanpoor, Aliofkhazraei, & Hamid Delavari, 2016). In addition, Zn has healing and bactericidal properties, which are enhanced by being in a matrix such as a zeolite with a large surface area (Rajendran, Kumar, Houreld, & Abrahamse, 2018).

The ion exchange of Zn in zeolites is a relatively simple process because Zn has a 2+ valence, allowing only a single oxidation state and a unique way of bonding to the zeolite structure. There are different works related to Zn ion exchange and the formation of nanoparticles (Almutairi, Mezari, Magusin, Pidko, & Hensen, 2012; Luzgin et al., 2008; Ostroski et al., 2009). However, no studies on the ion exchange of Zn in thermally modified zeolites have been reported.

In this work, the effect of Zn ion exchange in A4 zeolite modified by thermal treatment was studied to increase the surface area of the matrix (ZA4). The crystalline and molecular structures were defined by XRD and FTIR.

2 Materials and methods

Synthetic zeolite A4 (Sigma Aldrich, 98 %), zinc acetate $(CH_3COO)_2Zn.2H_2O$ (Sigma Aldrich, 99 %), and deionized water were used as the hydrates.

2.1 Thermally modified zeolite A4

Three samples with 12 grams of zeolite A4 were prepared, and sample 1 was thermally treated at 500 °C for 1 h. The second sample was thermally treated at 750 °C for 1 h. The third sample was thermally treated at 1000 °C for 1 h. All the samples were heated and cooled at a rate of 5 °C/min. These materials were named ZA4-500, ZA4-750 and ZA4-1000, respectively.

2.2 Thermally modified zeolite A4

For ZA4-500, the material was divided into 4 containers with 3 g, and 50 ml of distilled water each was added for hydration for 24 h. Afterwards, 3 solutions of 100 ml of $(CH_3COO)_2Zn.2H_2O$ were prepared at molarities of 0.01, 0.05, and 0.1 M. Then, hydrated zeolite and $(CH_3COO)_2Zn.2H_2O$ solutions were put in a thermal bath to obtain an internal temperature of 50 °C. After that, a solution of 0.01 M $(CH_3COO)_2Zn.2H_2O$ was slowly added to the container with hydrated zeolite. A solution of 0.05 M $(CH_3COO)_2Zn.2H_2O$ was slowly added to the container with hydrated zeolite. A 0.01 M solution of $(CH_3COO)_2Zn.2H_2O$ was slowly added to a vessel with hydrated zeolite. The final samples were filtered and dried at room temperature for 24 h. ZA4-500-0.01, ZA4-500-0.05, and ZA4-500-0.1 were obtained.

This process was repeated for ZA4-750 and ZA4-1000 under the same conditions, and the order of the nomenclature of the samples was maintained.

2.3 Characterization

XRD analysis was carried out with a PHI5100 BRUKER AXS D8 ADVANCE diffractometer. The vibrational energy of the bonds present in the structures of the different samples was determined by an IRAffinity 1-S Shimadzu Infrared Spectrometer. Micrographs and EDS results were measured with a JEOL JSM-7401F field emission scanning electron microscope (FESEM).

3 Results and discussion

Figure 1 shows the FT-IR spectra of ZA4 and ZA4-500, ZA4-750, and ZA4-1000. In ZA4, the peaks at 1655 and 3423 cm^{-1} are attributed to the distinctive vibrational stretching modes of the -OH bonds present in both chemical and physical water. Additionally, the peak at 1000 cm^{-1} is characteristic of the asymmetric stretching vibrations of Si-O-Si and Si-O-Al. The peak at 556 cm^{-1} indicates the symmetric stretching vibrations of the Si-O-Si and O-Si-O bonds, while the peak at 670 cm^{-1} corresponds to the asymmetric stretching vibrations of the Si-O-Al bonds (Mozgawa, Król, & Barczyk, 2011; Şen, Bardakçi, Yavuz, & Gök, 2008). For ZA4-500, the characteristic peaks of ZA4 are similar. However, the peak at 556 cm^{-1} shows a slight shift and the possible presence of a second peak near 500 cm^{-1}. This may be attributed to the effect of temperature on the modification of the molecular structure of ZA4; moreover, the peaks at 1655 and 3423 cm^{-1} are very small, which is caused by thermal treatment (Ates & Hardacre, 2012). For ZA4-750, the peak at 556 cm^{-1} shifted to 570 cm^{-1}, and the peak shifted to less than 500 cm^{-1}. In addition, peak formations are observed in the range of approximately 713 to 633 cm^{-1}, indicating possible molecular deformation in ZA4 (Aronne, Esposito, Ferone, Pansini, & Pernice, 2002; Yörükoğullar, Yilmaz, & Dikmen, 2010). These shifts and peak formations are more evident as the treatment temperature increases in ZA4; moreover, the peaks at 1665 and 3413 cm^{-1} disappear. For ZA4-1000, the peak at 558 cm^{-1} disappeared, which may indicate the breakdown of the D4R secondary structure, which is associated with that peak (Mozgawa et al., 2011), as well as the shift of the peak at 672 to 687 cm^{-1}, indicating possibly significant modification in the molecular structure of ZA4. Similarly, the peaks at 1665 and 3413 cm^{-1} disappeared after heat treatment. It can be observed that each of the thermal treatments applied to ZA4 caused the breakdown of SBU D4R, as indicated by the peak at 556 cm^{-1} (Flores-Valenzuela et al., 2023).

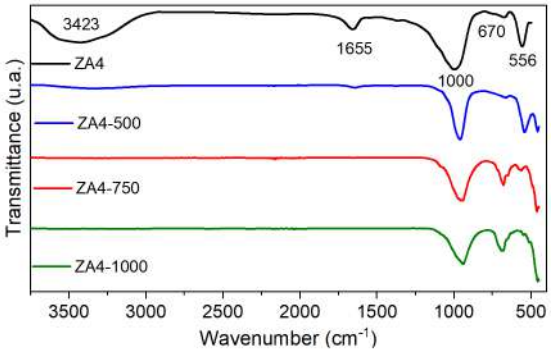

Figure 1. FT-IR spectra of ZA4, ZA4-500, ZA4-750, and ZA4-1000.

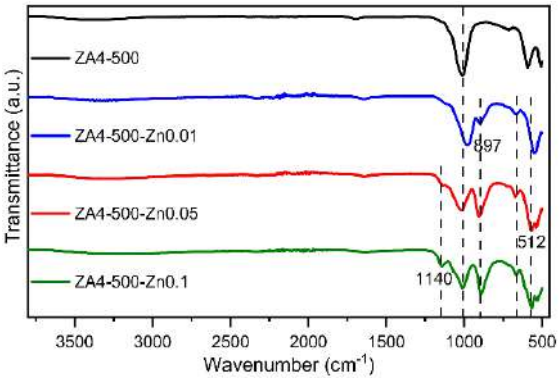

Figure 2. FT-IR spectra of ZA4-500, ZA4-500-Zn0.01, ZA4-500-Zn0.05, and ZA4-500-Zn0.1.

Figure 2 shows the FT-IR spectra of ZA4-500, ZA4-500-Zn0.01, ZA4-500-Zn0.05, and ZA4-500-Zn0.1. ZA4-500-Zn0.01 shows similar behavior to that of ZA4-500, with the presence of a new peak at 897 cm^{-1} attributed to the stretching modes of Zn-O (Ashokkumar & Muthukumaran, 2014). In addition, the peaks at 512 cm^{-1} for ZA4-500-Zn0.05 and ZA4-500-Zn0.1 are associated with the stretching modes of Zn-O to octahedral coordination and a possible increase in the degree of tetrahedral polymerization of SiO_4 (Ginting et al., 2019; Xiong, Pal, Serrano, Ucer, & Williams, 2006), as well as elongation of the peak at 897 $cm^{-1,}$ indicating a greater presence of Zn-O bonds (García-Molina et al., 2024). Another peak at 1141 cm^{-1} attributed to the normal polymeric O-H stretching vibration of H_2O in the Zn-O lattice is observed (Ashokkumar & Muthukumaran, 2014). These results provide evidence of alterations in the molecular structure of ZA4-500 due to changes in the Zn concentration.

Figure 3 shows the FT-IR spectra of ZA4-750, ZA4-750-Zn0.01, ZA4-750-Zn0.05 and ZA4-750-Zn0.1. The FT-IR spectra showed no apparent effect on the characteristic peak for ZA4-750; the peak at approximately 690 cm^{-1} was more intense; however, the FT-IR study was carried out qualitatively. Furthermore, the peak at 556 cm^{-1} disappears when ion exchange is carried out. Therefore, we can affirm

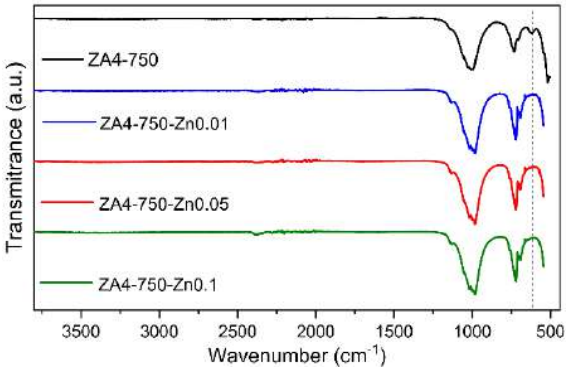

Figure 3. FT-IR spectra of ZA4-750, ZA4-750-Zn0.01, ZA4-750-Zn0.05 and ZA4-750-Zn0.1.

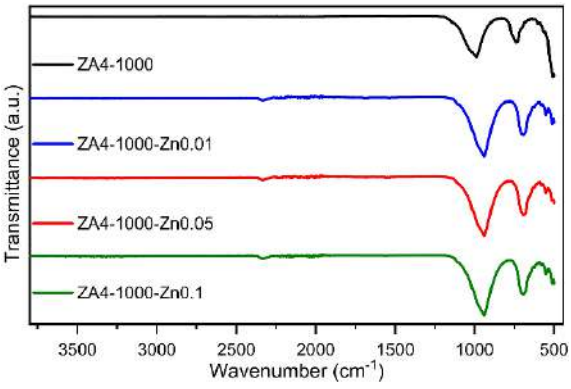

Figure 4. FT-IR spectra of ZA4-1000, ZA4-1000-Zn0.01, ZA4-1000-Zn0.05, and ZA4-1000-Zn0.1.

that the molecular structure of ZA4 thermally treated at 750 °C is affected by nanoparticle formation, ionic clusters or simple Zn ion exchange (Flores-Valenzuela et al., 2023; Ginting et al., 2019).

Figure 4 shows the FT-IR spectra of ZA4-1000, ZA4-1000-Zn0.01, ZA4-1000-Zn0.05, and ZA4-1000-Zn0.1. Under experimental conditions, the FR-IR spectra did not significantly change during ion exchange; therefore, we can conclude that ion exchange does not affect the molecular structure of ZA4 thermally treated at 1000 °C.

Figure 5 shows the X-ray diffraction patterns of ZA4, ZA4-500, ZA4-750 and ZA4-1000. The characteristic Miller indices of ZA4 are indicated by the solid line, indexed with card JCP2:01-089-5423. For ZA4-500, the same Miller indices characteristic of ZA4 were observed; however, a slight decrease in the intensity of the (220), (222) and (420) peaks was observed because of the heat treatment process applied to the zeolite. For ZA4-750, the characteristic peaks of ZA4 are observed, and new peaks at 21.3°, 24.6°, 29.4°, and 35.3° are also observed. According to the Miller indices, (003), (01-2), (01-3) and (01-4) belong to the "nepheline" group ($Na_{23.55}Al_{24}Si_{24}O_{96}$), which has a monoclinic structure and is indexed with PDF 96-901-0481. Nepheline is a porous tectosilicate with a chemical formula similar to that of ZA4. It presents

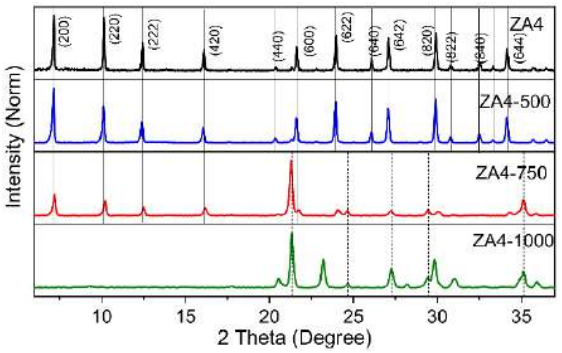

Figure 5. X-ray diffraction patterns of ZA4, ZA4-500, ZA4-750 and ZA4-1000.

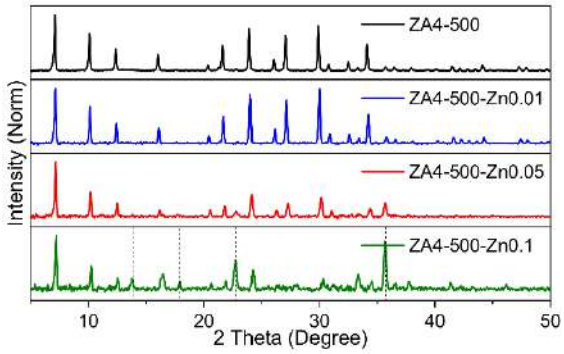

Figure 6. X-ray diffraction patterns of ZA4-500, ZA4-500-Zn0.01, ZA4-500-Zn0.05 and ZA4-500-Zn0.1.

a slight deficit of the element Na, creating a new structure. For ZA4-1000, only peaks for nepheline are observed, which may indicate that ZA4 changes to a monoclinic nepheline structure at high temperatures.

Figure 6 shows the X-ray diffraction patterns of ZA4-500, ZA4-500-Zn0.01, ZA4-500-Zn0.05 and ZA4-500-Zn0.1. For ZA4-500-Zn0.01, a similar behavior to that of ZA4-500 is observed, which may indicate that ion exchange at this concentration does not modify the crystalline properties of ZA4-500. For ZA4-500-Zn0.05, a similar behavior to that of ZA4-500 is observed; however, a decrease in the relative intensity of the peaks associated with Miller indices (220), (222) and (420) is evident. However, this peak could not be indexed to Zn^0 or ZnO; therefore, we may consider the formation of a forbidden plane in the zeolitic structure (He et al., 2015; Williams & Carter, 1996; Yan, Luo, Schaffer, & Qian, 2012). For ZA4-500-Zn0.1, a low peak resolution is observed, which can be interpreted as a tendency to transform the sample into an amorphous material, possibly caused by a high concentration of Zn in solution (Šponer, Sobalík, Leszczynski, & Wichterlová, 2001). Additionally, the crystallographic behavior is similar to that of ZA4-500-Zn0.05, where new peaks can be seen at 13.7° and 17.9°, which are not associated with any possible formation of nanoparticles. This is interpreted as the formation of forbidden planes. An increase in peak intensity is also observed at 22.9°

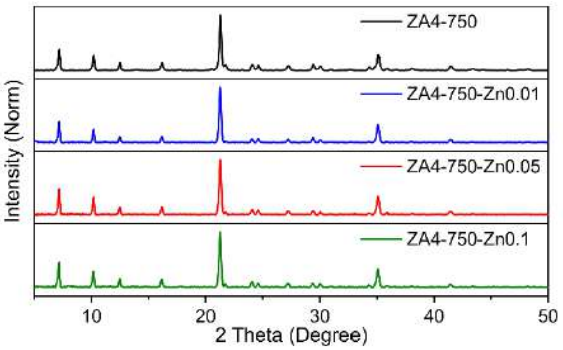

Figure 7. X-ray diffraction patterns of ZA4-750, ZA4-750-Zn0.01, ZA4-750-Zn0.05 and ZA4-750-Zn0.1.

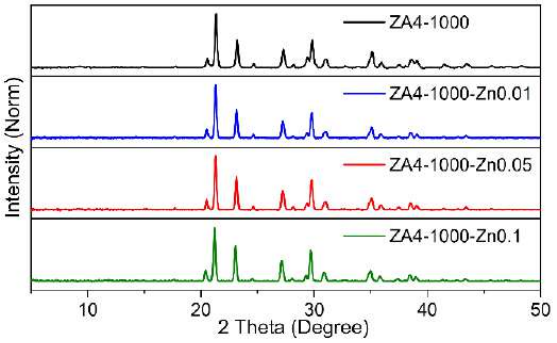

Figure 8. X-ray diffraction patterns of ZA4-1000, ZA4-1000-Zn0.01, ZA4-1000-Zn0.05, and ZA4-1000-Zn0.1.

and 36.7°, and the peak at 35.7° could be associated with the (101) plane of the ZnO nanoparticles (Borda, Torres, & Lapidus, 2022; Raoufi, 2013). However, this peak may be shielded by the ZA4 peak. For this sample, evidence of alteration in the crystal structure of ZA4-500 by ion exchange is observed.

Figure 7 shows the X-ray diffraction patterns of ZA4-750, ZA4-750-Zn0.01, ZA4-750-Zn0.05 and ZA4-750-Zn0.1. For these samples, the behavior of the crystalline structure is very similar and without apparent change for different concentrations. Therefore, we can determine that ion exchange does not affect the crystalline structure of ZA4-750; moreover, no evidence of characteristic peaks of nanoparticles is observed. Therefore, the formation of nanoparticles is absent or simply does not satisfy the diffraction criteria. (Warren, 1941; Whittig & Allardice, 2018).

Figure 8 shows the X-ray diffraction patterns of ZA4-1000, ZA4-1000-Zn0.01, ZA4-1000-Zn0.05, and ZA4-1000-Zn0.1. For those samples, the crystal structure behavior is very similar and without apparent variation for all concentrations, maintaining the nepheline structure. For this reason, we can reach the same conclusion as for ZA4-750, where we predict that ion exchange does not affect the crystalline structure of ZA4-1000 and that there is no evidence of characteristic peaks of nanoparticles.

Figure 9 shows the SEM and EDS micrographs for a) ZA4-500-Zn0.01, b) ZA4-500-Zn0.05 and c) ZA4-500-Zn0.1. For each sample, the morphology is similar and has no significant impact. However, EDS analysis shows that the atomic percentage of Zn for a) is 2.4 %, b) is 4.2 % and c) is 5.9 %. This is consistent due to the increasing Zn concentration in each sample. However, the Al/Si ratio was 1:1. However, variations in the molar concentration of the ion exchange result in changes in the Zn/Al ratio. Moreover, the samples for ZA4-750 and ZA4-1000 showed a low presence of Zn, lower than 0.5 atomic %, and therefore, this analysis was not included.

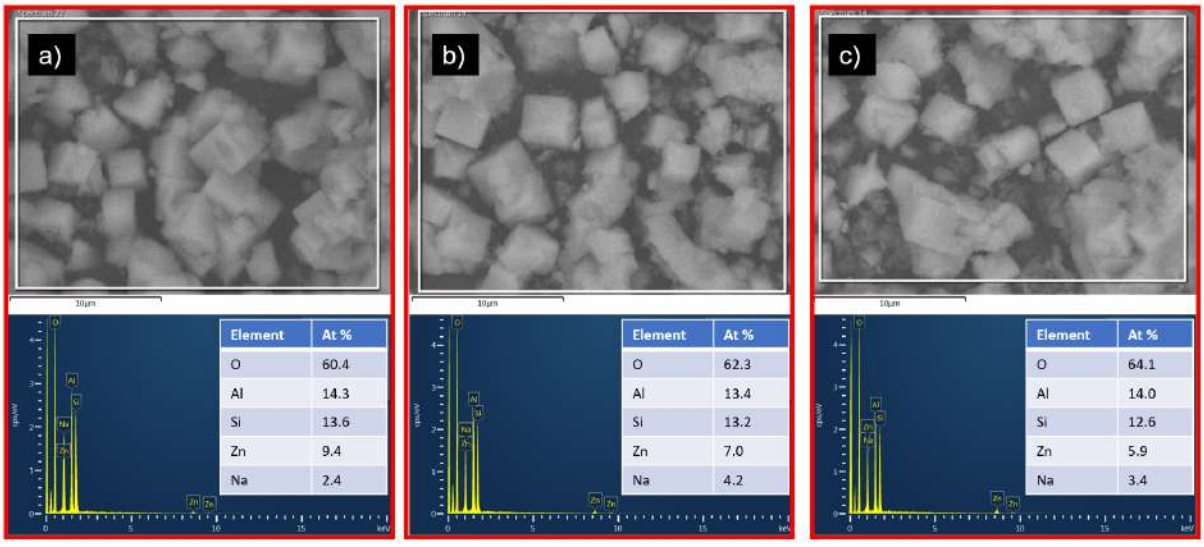

Figure 9. SEM and EDS images of a) ZA4-500-Zn0.01, b) ZA4-500-Zn0.05 and c) ZA4-500-Zn0.1.

Conclusion

FT-IR and XRD analyses showed significant molecular and crystalline structure modifications in zeolite due to heat treatment, as well as evidence of changes in each of the samples due to ion exchange. SEM micrographs showed no significant evidence of morphological variation. Additionally, the EDS analysis showed that heat treatment at 500 °C contributed to a greater ion exchange performance of Zn, which increased with increasing molar concentration. Furthermore, we conclude that heat treatments at 750 °C and 1000 °C cause phase transformations in the zeolite to nepheline, which is not suitable for ion exchange.

Importantly, the study of the structural and chemical properties of the thermally modified zeolite allows the prediction of different technological applications. This could be the formation of ZnO nanoparticles to be used as coatings in feed ovens where the elimination of bacteria harmful to the human body is required.

Acknowledgements

The authors acknowledge CONAHCYT and are thankful to members of staff at the Centro de investigación en Materiales Avanzados, S.C, Mexico, for the characterization and analysis. In addition, the technical support from R. P. Talamantes-Soto.

References

Almutairi, S. M. T., Mezari, B., Magusin, P. C. M. M., Pidko, E. A., & Hensen, E. J. M. (2012). Structure and reactivity of Zn-Modified ZSM-5 zeolites: The importance of clustered cationic Zn complexes. *ACS Catalysis*, *2*(1), 71–83. https://doi.org/10.1021/cs200441e

Aronne, A., Esposito, S., Ferone, C., Pansini, M., & Pernice, P. (2002). FTIR study of the thermal transformation of barium-exchanged zeolite A to celsian. *Journal of Materials Chemistry*, *12*(10), 3039–3045. https://doi.org/10.1039/b203859e

Ashokkumar, M., & Muthukumaran, S. (2014). Microstructure, optical and FTIR studies of Ni, Cu co-doped ZnO nanoparticles by co-precipitation method. *Optical Materials*, *37*(C), 671–678. https://doi.org/10.1016/j.optmat.2014.08.012

Ates, A., & Hardacre, C. (2012). The effect of various treatment conditions on natural zeolites: Ion exchange, acidic, thermal and steam treatments. *Journal of Colloid and Interface Science*, *372*(1), 130–140. https://doi.org/10.1016/j.jcis.2012.01.017

Borda, J., Torres, R., & Lapidus, G. (2022). Selective leaching of zinc and lead from electric arc furnace dust using citrate and H2SO4 solutions. A kinetic perspective. *Revista Mexicana de Ingeniera Quimica*, *21*(1). https://doi.org/10.24275/rmiq/cat2606

Breck, D. W., Eversole, W. G., & Milton, R. M. (1956). New synthetic crystalline zeolites. *Journal of the American Chemical Society*, *78*(10), 2338–2339. https://doi.org/10.1021/ja01591a082

Colella, C. (1996). Ion exchange equilibria in zeolite minerals. *Mineralium Deposita*, *31*(6), 554–562. https://doi.org/10.1007/BF00196136

Collins, F., Rozhkovskaya, A., Outram, J. G., & Millar, G. J. (2020). A critical review of waste resources, synthesis, and applications for Zeolite LTA. *Microporous and Mesoporous Materials*, *291*, 109667. https://doi.org/10.1016/j.micromeso.2019.109667

Eichhorn, H. (1858). On the reactions of silicates with dilute solutions of salts. *Pogendorf's. Ann. Phys*, *105*, 126.

Eroglu, N., Emekci, M., & Athanassiou, C. G. (2017, August 1). Applications of natural zeolites on agriculture and food production. *Journal of the Science of Food and Agriculture*. John Wiley & Sons, Ltd. https://doi.org/10.1002/jsfa.8312

Flores-Valenzuela, J., Leal-Perez, J. E., Almaral-Sanchez, J. L., Hurtado-Macias, A., Borquez-Mendivil, A., Vargas-Ortiz, R. A., … Cortez-Valadez, M. (2023). Structural Analysis of Cu+ and Cu2+ Ions in Zeolite as a Nanoreactor with Antibacterial Applications. *ACS Omega*, *4*, 0. https://doi.org/10.1021/acsomega.3c03869

Gans, R. (1905). Zeolites and similar compounds, their constitution and meaning for technology and agriculture. *Jahrbuch Der Königlich Preussischen Geologischen Landesanstalt*, *26*, 179.

García-Molina, R., Suárez-Velázquez, G. G., Pech-Rodríguez, W. J., Ordóñez, L. C., Melendez-Gonzalez, P. C., Sánchez-Padilla, N. M., & González-Quijano, D. (2024). Soft chemistry synthesis of size-controlled ZnO nanostructures as photoanode for dye-sensitized solar cell.

Revista Mexicana de Ingeniería Química, *23*(2), IE24235. https://doi.org/https://doi.org/10.24275/rmiq/IE24235

Ginting, S. B., Yulia, Y., Wardono, H., Darmansyah, Hanif, M., & Iryani, D. A. (2019). Synthesis and Characterization of Zeolite Lynde Type A (LTA): Effect of Aging Time. In *Journal of Physics: Conference Series* (Vol. 1376, p. 012041). IOP Publishing. https://doi.org/10.1088/1742-6596/1376/1/012041

Hasanpoor, M., Aliofkhazraei, M., & Hamid Delavari, H. (2016). In-situ study of mass and current density for electrophoretic deposition of zinc oxide nanoparticles. *Ceramics International*, *42*(6), 6906–6913. https://doi.org/10.1016/j.ceramint.2016.01.076

He, M., Liu, T. Z., Qiu, M. H., Zhang, Z. H., Zhu, Y. Z., Song, Z., & Xiu, J. L. (2015). Study on the optical properties of ErBa3B9O18crystals. *Physica B: Condensed Matter*, *456*, 100–102. https://doi.org/10.1016/j.physb.2014.08.037

Hoveyda, A. H., & Zhugralin, A. R. (2007, November 8). The remarkable metal-catalysed olefin metathesis reaction. *Nature*. Nature Publishing Group. https://doi.org/10.1038/nature06351

Julbe, A., & Drobek, M. (2016). Zeolite T Type. *Encyclopedia of Membranes*, 2058–2059. https://doi.org/10.1007/978-3-662-44324-8_606

Leal-Perez, J. E., Flores-Valenzuela, J., Cortez-Valadez, M., Hurtado-Macías, A., Vargas-Ortiz, R. A., Bocarando-Chacon, J. G., & Almaral-Sánchez, J. L. (2022). Optical properties of copper clusters in zeolite 4A with surface enhanced Raman spectroscopy applications. *Applied Physics A: Materials Science and Processing*, *128*(8), 649. https://doi.org/10.1007/s00339-022-05785-6

Leal-Perez, J. E., Flores-Valenzuela, J., Vargas-Ortíz, R. A., Alvarado-Beltrán, C. G., Hurtado-Macias, A., & Almaral-Sánchez, J. L. (2022). Synthesis of Cu2S Ultrasmall Nanoparticles in Zeolite 4A Nanoreactor. *Journal of Cluster Science*, 1–6. https://doi.org/10.1007/s10876-022-02330-6

Luzgin, M. V., Rogov, V. A., Arzumanov, S. S., Toktarev, A. V., Stepanov, A. G., & Parmon, V. N. (2008). Understanding Methane Aromatization on a Zn-Modified High-Silica Zeolite. *Angewandte Chemie*, *120*(24), 4635–4638. https://doi.org/10.1002/ange.200800317

Mozgawa, W., Król, M., & Barczyk, K. (2011). FT-IR studies of zeolites from different structural groups. *Chemik*, *65*(7), 671–674.

Ostroski, I. C., Barros, M. A. S. D., Silva, E. A., Dantas, J. H., Arroyo, P. A., & Lima, O. C. M. (2009). A comparative study for the ion exchange of Fe(III) and Zn(II) on zeolite NaY. *Journal of Hazardous Materials*, *161*(2–3), 1404–1412. https://doi.org/10.1016/j.jhazmat.2008.04.111

Rajendran, N. K., Kumar, S. S. D., Houreld, N. N., & Abrahamse, H. (2018). A review on nanoparticle based treatment for wound healing. *Journal of Drug Delivery Science and Technology*, *44*, 421–430. https://doi.org/10.1016/j.jddst.2018.01.009

Raoufi, D. (2013). Synthesis and microstructural properties of ZnO nanoparticles prepared by precipitation method. *Renewable Energy*, *50*, 932–937. https://doi.org/10.1016/j.renene.2012.08.076

Reyes-Zambrano, S. J., Lecona-Guzmán, C. A., Luján-Hidalgo, M. C., & Gutiérrez-Miceli, F. A. (2024). Stimulation of morphometric parameters and zinc content of native maize by priming with zinc oxide phytonanoparticles. *Revista Mexicana de Ingeniería Química*, *23*(1), 1–12. https://doi.org/10.24275/rmiq/bio24160

Şen, S., Bardakçi, B., Yavuz, A. G., & Gök, A. U. (2008). Polyfuran/zeolite LTA composites and adsorption properties. *European Polymer Journal*, *44*(8), 2708–2717. https://doi.org/10.1016/j.eurpolymj.2008.05.018

Šponer, J. E., Sobalík, Z., Leszczynski, J., & Wichterlová, B. (2001). Effect of metal coordination on the charge distribution over the cation binding sites of zeolites. A combined experimental and theoretical study. *Journal of Physical Chemistry B*, *105*(35), 8285–8290. https://doi.org/10.1021/jp010098j

Warren, B. E. (1941). X-ray diffraction methods. *Journal of Applied Physics*, *12*(5), 375–383. https://doi.org/10.1063/1.1712915

Whittig, L. D., & Allardice, W. R. (2018). X-ray diffraction techniques. In *Methods of Soil Analysis, Part 1: Physical and Mineralogical Methods* (pp. 331–362). John Wiley & Sons, Ltd. https://doi.org/10.2136/sssabookser5.1.2ed.c12

Williams, D. B., & Carter, C. B. (1996). The Transmission Electron Microscope. In *Transmission Electron Microscopy* (pp. 3–17). Springer, Boston, MA. https://doi.org/10.1007/978-1-4757-2519-3_1

Xiong, G., Pal, U., Serrano, J. G., Ucer, K. B., & Williams, R. T. (2006). Photoluminesence and FTIR study of ZnO nanoparticles: the impurity and defect perspective. *Physica Status Solidi C*, *3*(10), 3577–3581. https://doi.org/10.1002/pssc.200672164

Yan, M., Luo, S. D., Schaffer, G. B., & Qian, M. (2012). TEM and XRD characterisation of commercially pure α-Ti made by powder metallurgy and casting. *Materials Letters*, *72*, 64–67. https://doi.org/10.1016/j.matlet.2011.12.072

Yörükoğullar, E., Yilmaz, G., & Dikmen, S. (2010). Thermal treatment of zeolitic tuff. In *Journal of Thermal Analysis and Calorimetry* (Vol. 100, pp. 925–928). Akadémiai Kiadó, co-published with Springer Science+Business Media B.V., Formerly Kluwer Academic Publishers B.V. https://doi.org/10.1007/s10973-009-0503-8